Supporting information for

Carrier Transport Composites with Suppressed Glass-Transition for Stable Planar Perovskite Solar Cells

Ligang Wang,[a] Huanping Zhou,*[,a] Nengxu Li,[a] Yu Zhang, [a] Lihaokun Chen,[a] Xiaoxing Ke,[b] Zhenxin Chen,[b] Zelin Wang,[b] Manling Sui,[b] Yihua Chen,[a] Yuan Huang,[a] Liang Li,[a] Ziqi Xu,[a] Qi Chen,[c] Ling-Dong Sun,*[a] Chun-Hua Yan*[a, d]

[a] Beijing National Laboratory for Molecular Sciences, State Key Laboratory of Rare Earth Materials Chemistry and Applications, PKU-HKU Joint Laboratory in Rare Earth Materials and Bioinorganic Chemistry, Key Laboratory for the Physics and Chemistry of Nanodevices, Beijing Key Laboratory for Theory and Technology of Advanced Battery Materials, Department of Materials Science and Engineering, College of Engineering, College of Chemistry and Molecular Engineering, Peking University, Beijing 100871, P. R. China.

[b] Institute of Microstructure and Property of Advanced Materials, Beijing University of Technology, Beijing 100124, P. R. China.

[c] Department of Materials Science and Engineering, Beijing Institute of Technology, Beijing 100081, P. R. China

[d] College of Chemistry and Chemical Engineering, Lanzhou University, Lanzhou 730000, P. R. China.

Corresponding Author:
* Prof. H. P. Zhou. E-mail: happy_zhou@pku.edu.cn
* Prof. L. D. Sun. E-mail: sun@pku.edu.cn
* Prof. C. H. Yan. E-mail: yan@pku.edu.cn

Materials:

All reagents were used as received without further purification. CsI (99.9%, Sigma-Aldrich), $PbCl_2$ (99.99%, Aladdin), $PbBr_2$ (99%, Aladdin), PbI_2 (99.999%, Sigma-Aldrich), formamidine acetate (99%, Aladdin), methylamine (ethanol solution 28%w, Sinopharm), HCl (37%w, Xilong Scientific), HBr (41%w, Sinopharm), HI (45%w, Xilong Scientific), polymer poly(triarylamine) (PTAA, 99%, Xi'an Polymer Light Technology Corp.), [2,2′,7,7′-tetrakis (N,N-di-p-methoxyphenyl-amine) 9,9′-spirobifluorene] (spiro-OMeTAD, 99%, Xi'an Polymer Light Technology Corp.), 4-tert-butylpyridine (tBP, 99.9%, Sigma-Aldrich), lithium bis(trifluoromethanesulfonyl) imide (LiTFSI, 99.95% Sigma-Aldrich), acetonitrile (99.95%, Sigma-Aldrich), SnO_2 colloid precursor (15% in H_2O, Alfa Aesar), diethyl ether (AR), chlorobenzene (CB, 99.9%, Sigma-Aldrich), N,N-dimethylformamide (DMF, 99.99%, Sigma-Aldrich), dimethylsulfoxide (DMSO, 99.99%, Sigma-Aldrich), acetonitrile (99.9%, Sigma-Aldrich), isopropanol (IPA, 99.99%, Sigma-Aldrich). Indium tin oxide substrate (ITO, Yingkou youxuan Trade Co. Ltd). FAI, MACl, MABr, MAI were synthesized according to the reported method which can be seen everywhere.[1] MA is methylammonium and FA is formamidinium.

Devices preparation:

Typical planar n-i-p perovskite solar cells (PSCs) with ITO/SnO_2/perovskite/hole transport material (HTM)/Au structure were prepared as follows: ITO (10 Ω/□) coated glass substrates were washed by ultrasonic scrubber in deionized water, acetone, IPA sequentially. Before SnO_2 deposition, the substrate was cleaned by UV-O_3 cleaner for 20 min. SnO_2 nanoparticles dispersion solution was diluted to 2.0%w before deposition, then deposited by spin coating at 4000 r·min^{-1}, followed annealing process at 150 °C for 30 min in air. Perovskite layer was deposited in air by a typical two-step deposition method. Two type of perovskite layers with little component difference were used for verifying its universality and effectiveness of SMPHTC and obtaining stable and efficient planar PSCs. Two type perovskite layers prepared by same first step and same precursor components for PbX_2 layer. Firstly, inorganic PbX_2 layer (CsI 20 mg, PbI_2 540 mg, $PbBr_2$ 20 mg, $PbCl_2$ 20 mg, MAI 5 mg and 0.15% europium(Ⅲ) acetylacetonate ($Eu(acac)_3$ for constant elimination of Pb^0 and I^0 defects in PSCs, Eu/Pb, molar ratio)[2] were dissolved in 870 μL DMF and 130 μL DMSO mixed solvent) was prepared by spin-coating at 2,600 r·min^{-1} for 30 s, and annealed at 70 °C for 1 min. One type of perovskite layer was prepared with cation isopropanol (IPA) solution (20 mg MAI 40 mg FAI, 3 mg MABr and 5 mg MACl were dissolved in 1 mL IPA, $Cs_{0.06}FA_{0.58}MA_{0.36}I_{2.88}Br_{0.12}(Cl)$ perovskite) was spin-coated on PbX_2 layer at 2,100 r·min^{-1} for 30 s, then followed a annealing process at 145 °C for 15 min. MA is thermally less stable than FA. To achieve better thermal stability, MAI was mostly replaced by FAI (5 mg MAI 55 mg FAI, 3 mg MABr and 5 mg MACl, $Cs_{0.06}FA_{0.87}MA_{0.07}I_{2.88}Br_{0.12}(Cl)$ perovskite) in another type perovskite layer for both phase and thermal stability requirement. The different ratio hole-transport material solution was prepared by directly mixing a given volume ratio of spiro-OMeTAD and PTAA solution (defined as S_xP_y, such as 1:1 volume ratio spiro-OMeTAD: PTAA defined as S_1P_1). Spiro-OMeTAD (80 mg·mL^{-1} in chlorobenzene) solution contains tBP (35 uL·mL^{-1}), LiTFSI (30 μL·mL^{-1}, 270 mg·mL^{-1} dissolved in acetonitrile) and PTAA (10 mg·mL^{-1} in chlorobenzene) contains tBP (5 μL·mL^{-1}), LiTFSI (5 μL·mL^{-1}, 270 mg·mL^{-1} dissolved in acetonitrile) additives. Hole transport layer was deposited by spin coating at 2,500 r·min^{-1} for 30 s. Then, the cells were stored for further oxidation in oxygen filled box for 12 h. 80 nm gold electrodes were deposited by thermal evaporation under 10^{-5} Pa.

Characterization

Solar cell characterization

The current density-voltage (*J-V*) curves of solar cells were obtained by a source meter (Keithley 2400) with a solar simulator (Newport, Oriel Class A, 91195A) at 1000 $W \cdot m^{-2}$ illumination (AM 1.5 G) calibrated by a Si reference cell certified by NREL. The *J-V* curves were obtained by reverse (1.2 V to −0.2 V) or forward (−0.2 V to 1.2 V) scanning modes. The J–V curves of each device were measured by masking the active area with a metal mask (certified area, 0.09408 cm^2). The MPP data at room temperature (25 °C) was obtained without encapsulation and cooling in the nitrogen-filled glove box, and continuously recorded by a home-made equipment consisting of electrochemical workstation and software. The MPP at 85 °C was also obtained by continuous tracking without interruption in the nitrogen-filled glove box, and measured by source meter (Keithley 2400) on 85 °C hotplate, and the data were recorded by directly reading the parameters in the source meter every several hours

Scanning electron microscope (SEM)

SEM images was obtained with field emission scanning electron microscope (2 KeV, MERLIN Compact, ZEISS Germany).

Fourier Transform Infrared Spectroscopy (FTIR)

Samples were prepared with KBr pellet. FTIR was obtained by Magna-IR 750 (Nicolet, USA).

Time-resolved photoluminescence (TRPL) and photoluminescence (PL)

Perovskite coated with/without HTM samples were prepared on glass substrate. Characterization was performed at 780 nm with 470 nm excitation on FLS980 (Edinburgh Instruments Ltd.).

Electrochemical impedance spectroscopy (EIS)

EIS was performed on PSCs with ITO/SnO_2/perovskite/HTM/Au structure, and obtained by using an electrochemical workstation (Germany, Zahner Company). EIS spectra were recorded under 1-sun illumination in the frequency range from 10^6 to 1 Hz with an AC amplitude of 50 mV.at room temperature (25 °C) in 1-sun illumination (AM 1.5 G, 1000 $W \cdot m^{-2}$).

X-ray diffraction (XRD) characterization

The perovskite samples were made by depositing perovskite films on the glass substrates. XRD patterns were performed using X-ray powder diffractometer with Cu Kα radiation (PANalytical X'Pert Pro, $\lambda = 1.54050$ Å)

Photoelectron Spectrometer (PESA) in air

The samples were prepared on the ITO substrates. PESA was performed in air on low energy Photoelectron Spectrometer AC-2 (Riken Keiki, Japan) to measure the ionization potentials or highest occupied molecular orbital (HOMO) energy levels.

Thermogravimetric analysis (TGA) and differential scanning calorimetry (DSC)

Simultaneous TGA-DSC was recorded on a SDT Q600 instrument (TA Instruments, Japan) under

a nitrogen gas flow of 100 mL·min^{-1} and using a 5 °C·min^{-1} temperature increase rate.

Photo-thermal infrared spectroscopy (PTIR)

HTM layer samples were prepared on ITO/perovskite substrate. Characterizations were performed at Shanghai NTI Co., Ltd. on Photo-induced Force Microscopy instrument (USA, VistaScope, <10 nm spatial resolution and superfast nanoscale IR spectroscopy < 0.1 s for full spectrum). IR spectra was collected in infrared molecular fingerprint region (770 - 1885 cm^{-1})

High-angle annular dark-field imaging (HAADF) scanning transmission electron microscope (STEM)

Aged PSCs were cut by using focused ion beam (FIB) cutting instrument to get cross-section images. Images was obtained by Titan G2 (FEI) TEM instrument equipped with an aberration corrector for probe forming lens.

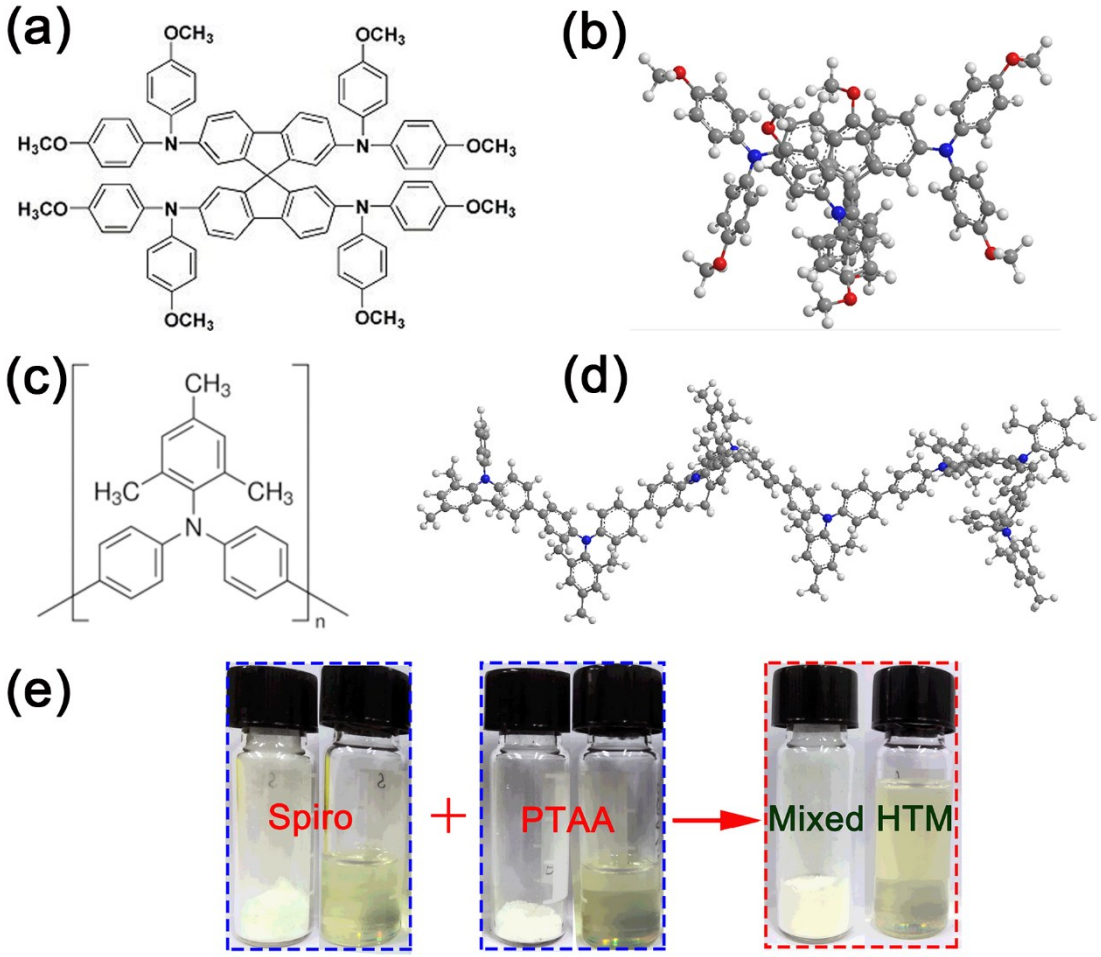

Figure S1. (a) Molecule structure and (b) ball-and-stick model of spiro-OMeTAD. (c) Molecule structure and (d) ball-and-stick model of PTAA (8 units). (e) Solid and solution of spiro-OMeTAD, PTAA and SMPHTC.

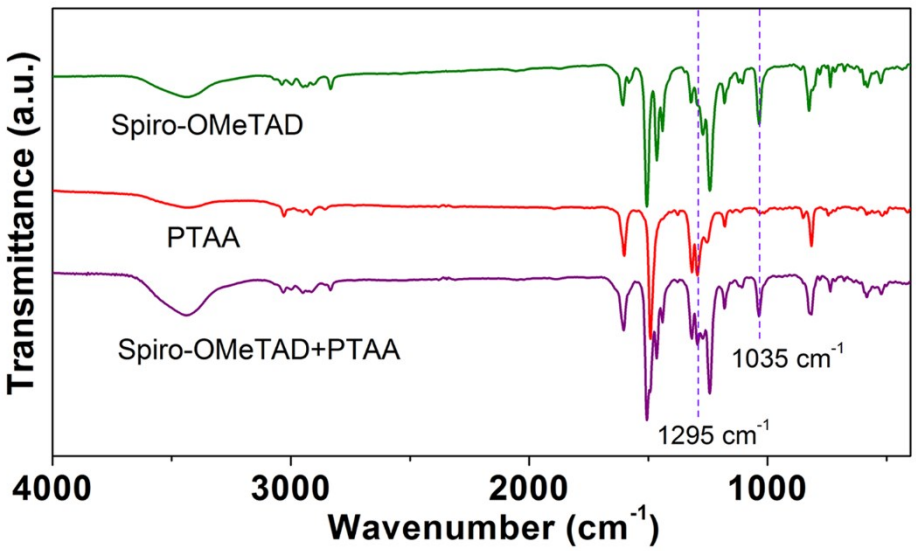

Figure S2. FTIR absorption spectra of spiro-OMeTAD, PTAA and mixture from KBr pellet.

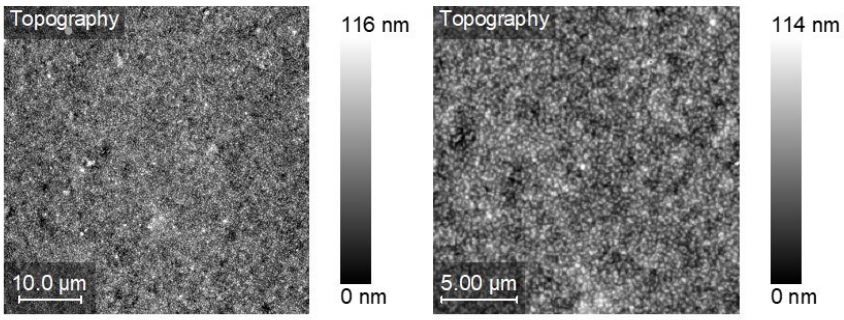

Figure S3. Large area topography images of S_1P_1 film. 50 × 50 µm^2 and 20 × 20 µm^2.

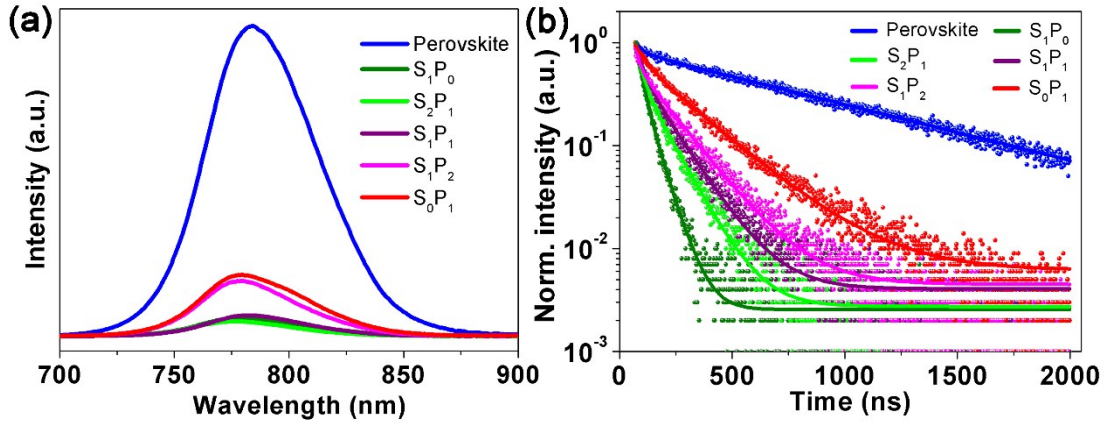

Figure S4. (a) Photoluminescence spectrum. (b) Time-resolved photoluminescence (excited by 470 nm pulse laser) of $Cs_{0.06}FA_{0.58}MA_{0.36}I_{2.88}Br_{0.12}(Cl)$ perovskite film coated with different ratio spiro-OMeTAD/PTAA.

Table S1. Fitted result of time-resolved photoluminescence (excited by 470 nm pulse laser) of $Cs_{0.06}FA_{0.58}MA_{0.36}I_{2.88}Br_{0.12}(Cl)$ perovskite film coated with different ratio spiro-OMeTAD/PTAA.

HTMs	**τ_1 (ns)**	**τ_2 (ns)**	**R^2**
Perovskite	42.7	801	0.993
S_1P_0	23.1	59.8	0.998
S_2P_1	24.8	105	0.997
S_1P_1	30.9	127	0.997
S_1P_2	35.8	156	0.995
S_0P_1	48.3	235	0.997

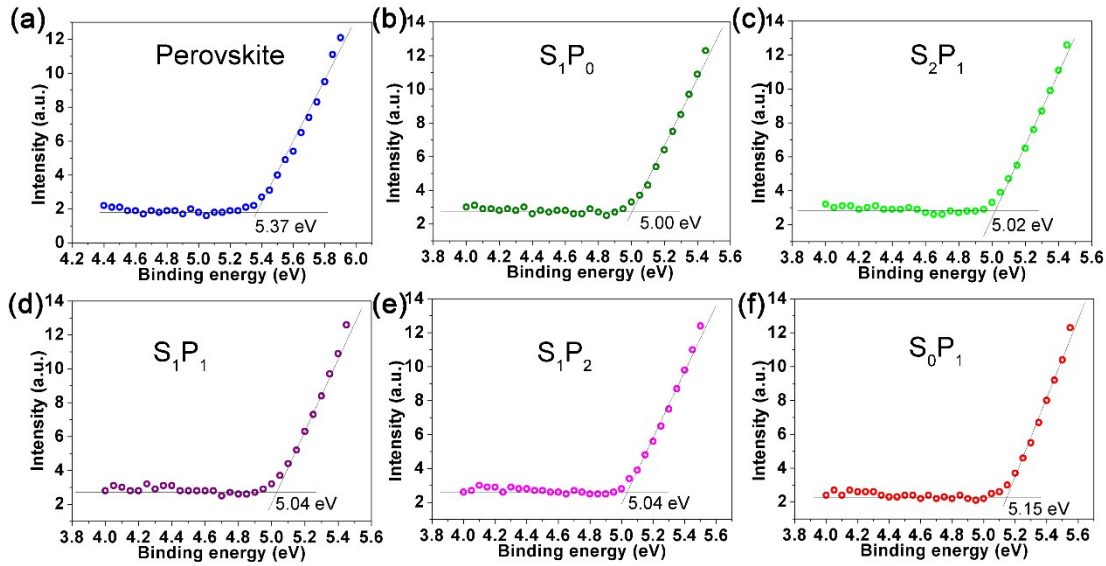

Figure S5. Photoelectron spectrometer (PESA) spectra of different ratio spiro-OMeTAD/PTAA HTMs. (a) $Cs_{0.06}FA_{0.58}MA_{0.36}I_{2.88}Br_{0.12}(Cl)$ perovskite (b) S_1P_0, (c) S_2P_1, (d) S_1P_1, (e) S_1P_2, (f) S_0P_1. Coated on ITO substrate.

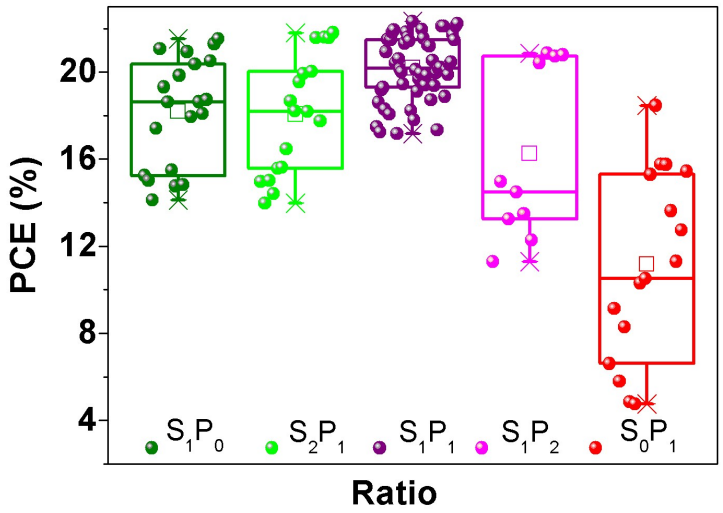

Figure S6. (a) Original PCE distribution of different ratio spiro-OMeTAD/PTAA layer based $Cs_{0.06}FA_{0.87}MA_{0.07}I_{2.88}Br_{0.12}(Cl)$ PSCs.

Table S2. Photovoltaic parameters of $Cs_{0.06}FA_{0.87}MA_{0.07}I_{2.88}Br_{0.12}(Cl)$ PSCs with different ratio spiro-OMeTAD/PTAA HTMs.

HTMs	V_{OC} (V)	J_{SC} (mA·cm^{-2})	FF (%)	PCE (%)
S_1P_0	1.09 ± 0.04	23.6 ± 0.6	70.7 ± 8.2	18.2 ± 2.4
S_2P_1	1.05 ± 0.05	23.6 ± 0.8	72.4 ± 6.6	18.1 ± 2.6
S_1P_1	1.12 ± 0.03	23.8 ± 0.5	76.1 ± 4.3	20.2 ± 1.5
S_1P_2	1.06 ± 0.06	23.0 ± 0.7	66.3 ± 10.8	16.3 ± 3.8
S_0P_1	0.96 ± 0.05	21.1 ± 3.0	53.4 ± 12.8	11.2 ± 4.2

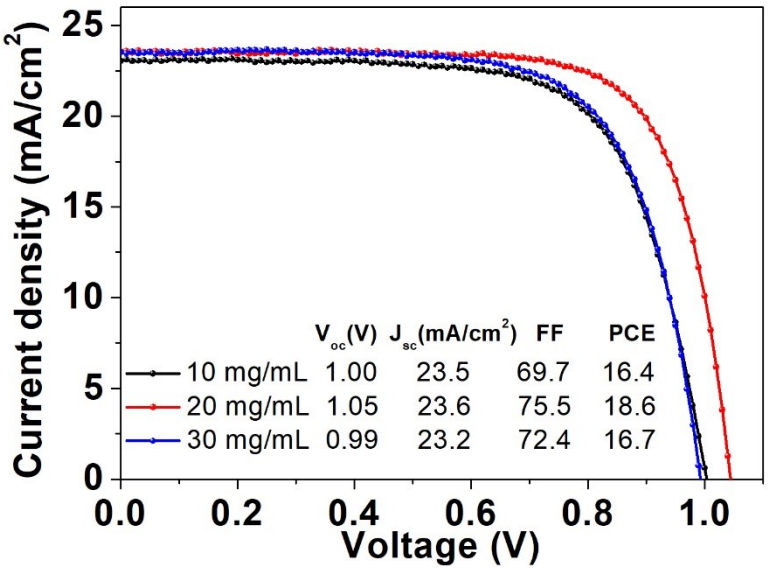

Figure S7. Representative *J-V* curves and parameters of the $Cs_{0.06}FA_{0.58}MA_{0.36}I_{2.88}Br_{0.12}(Cl)$ PSCs based on different concentration of pure PTAA solution dissolved in chlorobenzene.

Table S3. Photovoltaic parameters of $Cs_{0.06}FA_{0.58}MA_{0.36}I_{2.88}Br_{0.12}(Cl)$ PSCs based on different concentration PTAA HTMs.

HTMs	**V_{OC} (V)**	**J_{SC} (mA·cm^{-2})**	**FF (%)**	**PCE (%)**
S_0P_1 20 mg·mL^{-1}	1.03 ± 0.02	23.5 ± 0.3	67.9 ± 9.9	16.4 ± 2.7
S_0P_1 30 mg·mL^{-1}	0.95 ± 0.04	17.3 ± 1.3	69.0 ± 2.2	7.2 ± 2.2

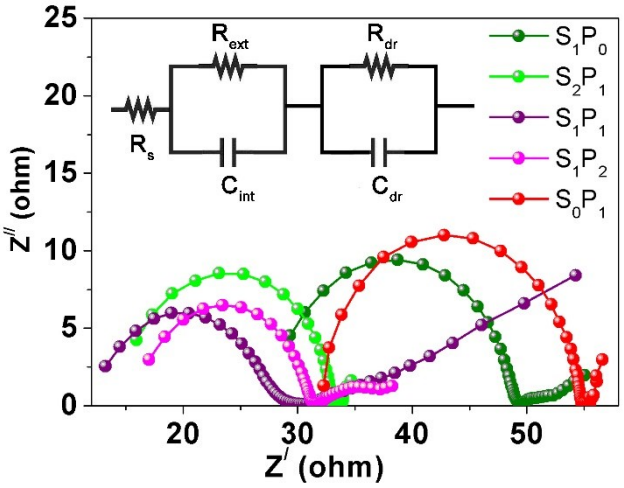

Figure S8. Nyquist plots of $Cs_{0.06}FA_{0.58}MA_{0.36}I_{2.88}Br_{0.12}(Cl)$ PSCs with different ratio spiro-OMeTAD/PTAA measured by EIS under 1-sun illumination, the insertion is the equivalent circuit.

Table S4. Fitted results in EIS measurements of different ratio spiro-OMeTAD/PTAA layer based $Cs_{0.06}FA_{0.58}MA_{0.36}I_{2.88}Br_{0.12}$(Cl) PSCs.

HTMs	R_s (ohm)	R_{ext} (ohm)	R_{dr} (ohm)
S_1P_0	28.2	19.7	29.6
S_2P_1	15.1	19.0	40.5
S_1P_1	13.5	14.2	79.3
S_1P_2	16.5	13.9	35.8
S_0P_1	31.2	22.3	32.7

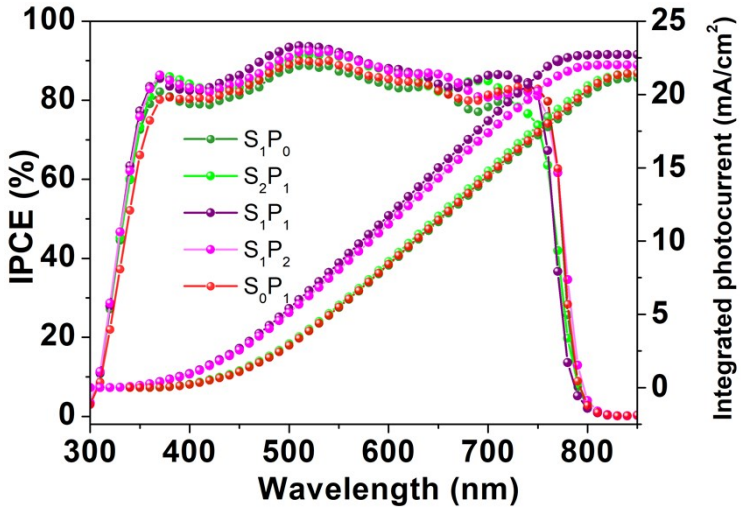

Figure S9. Incident photon-to-current efficiency (IPCE) of different ratio spiro-OMeTAD/PTAA layer based $Cs_{0.06}FA_{0.58}MA_{0.36}I_{2.88}Br_{0.12}$(Cl) PSCs.

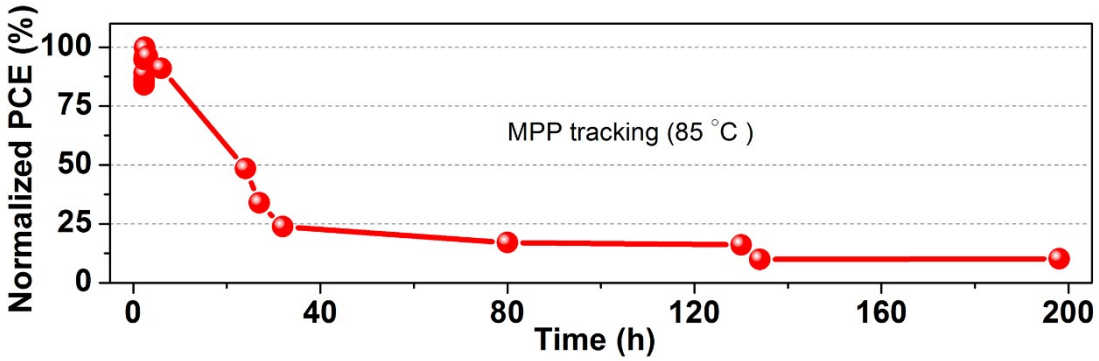

Figure S10. The stabilized power output (SPO) tracking at initial maximum power point (MPP) voltage of the S_1P_1 HTM-based $Cs_{0.06}FA_{0.87}MA_{0.07}I_{2.88}Br_{0.12}$(Cl) PSCs, measured at 0.97 V by source meter (Keithley 2400) at 85 °C and 1-sun illumination, the original PCE is 19.2%. The un-encapsulated PSC was placed on 85 °C hot plate and parameters were recorded every dozens of hours.

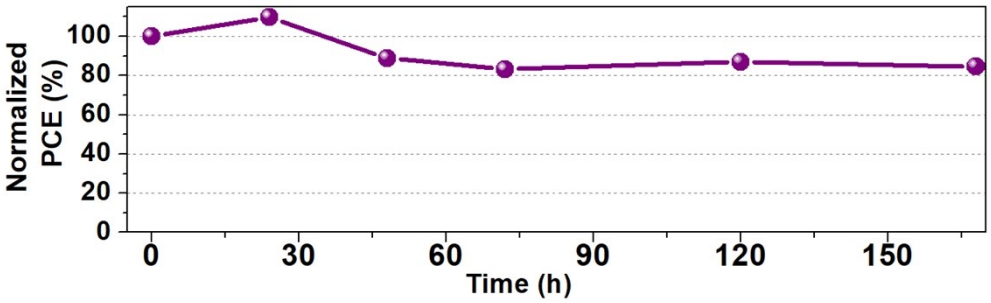

Figure S11. PCE evaluation under 85 °C of S_1P_1 based $Cs_{0.06}FA_{0.58}MA_{0.36}I_{2.88}Br_{0.12}$(Cl) PSCs. The original average PCE is 17.5%.

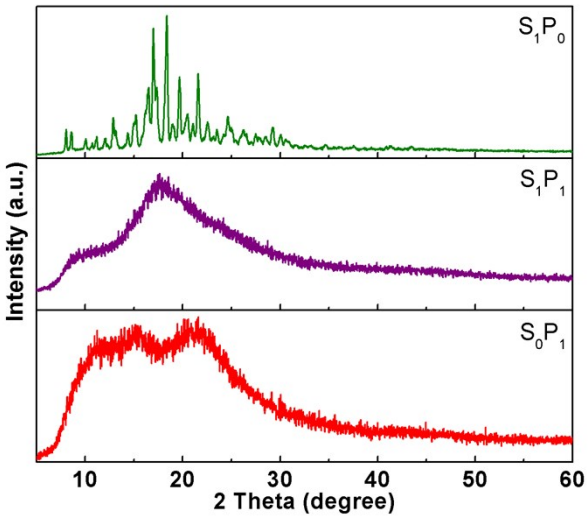

Figure S12. XRD of S_1P_0, S_1P_1 and S_0P_1 HTMs solid powder.

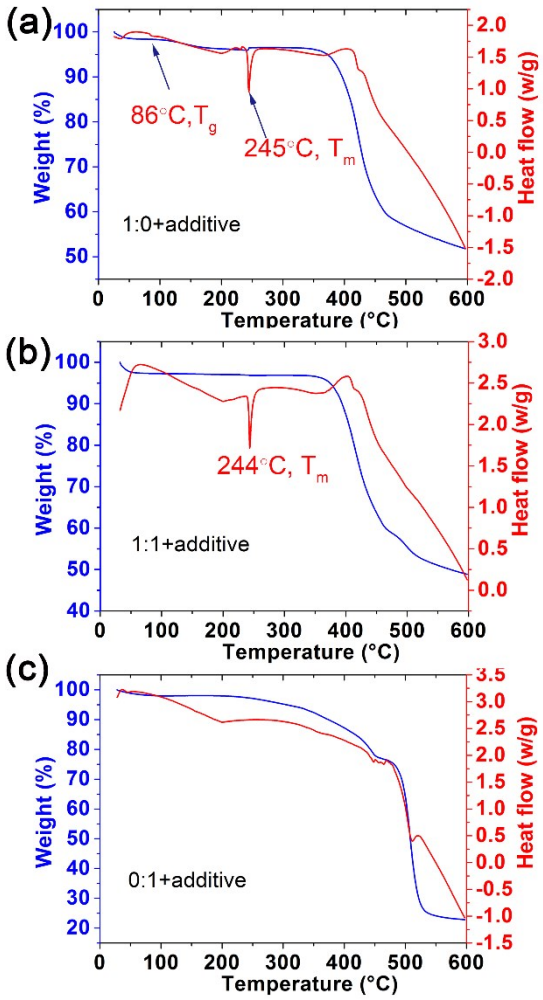

Figure S13. TGA-DSC of (a) S_1P_0, (b) S_1P_1 and (c) S_0P_1 HTMs powder.

Table S5. Thickness tested by step profiler of HTM layers prepared with different ratio composite and different concentration PTAA.

HTMs	thickness (nm)
S_1P_0	285
S_2P_1	176
S_1P_1	143
S_1P_2	106
S_0P_1 10 mg·mL^{-1}	44
S_0P_1 20 mg·mL^{-1}	92
S_0P_1 30 mg·mL^{-1}	154
S_0P_1 40 mg·mL^{-1}	223
S_0P_1 50 mg·mL^{-1}	416

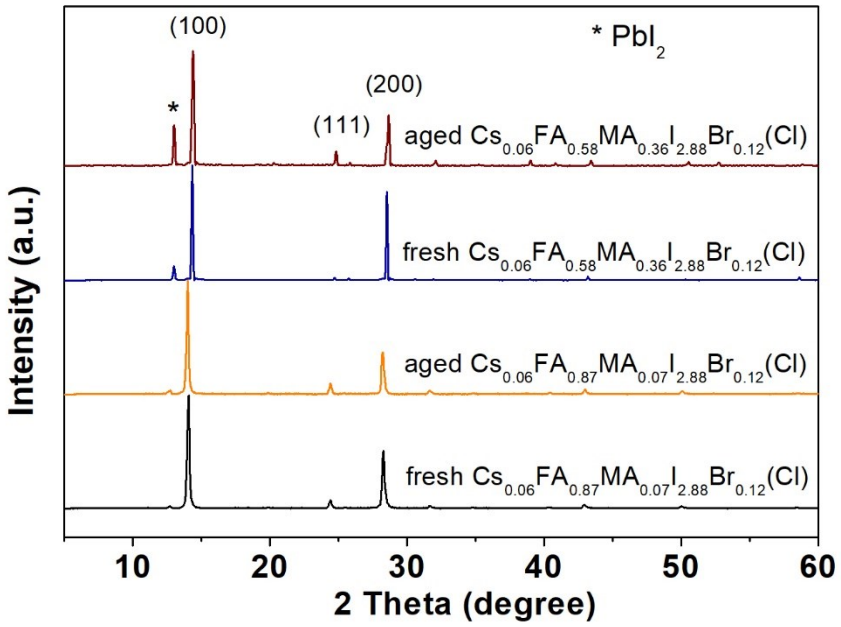

Figure S14. XRD of fresh and aged $Cs_{0.06}FA_{0.87}MA_{0.07}I_{2.88}Br_{0.12}(Cl)$ and $Cs_{0.06}FA_{0.58}MA_{0.36}I_{2.88}Br_{0.12}(Cl)$ perovskite films. Aging condition is 85 °C for 1000 h.

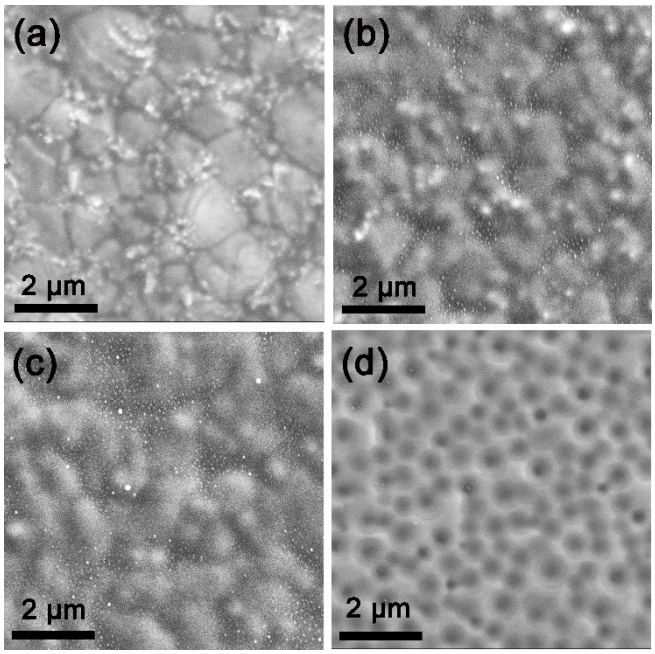

Figure S15. SEM images of PTAA films prepared by different concentration solution. (a) 20 $mg \cdot mL^{-1}$, (b) 30 $mg \cdot mL^{-1}$, (c) 40 $mg \cdot mL^{-1}$, (d) 50 $mg \cdot mL^{-1}$ PTAA solution spin-coated on $Cs_{0.06}FA_{0.58}MA_{0.36}I_{2.88}Br_{0.12}(Cl)$ perovskite film.

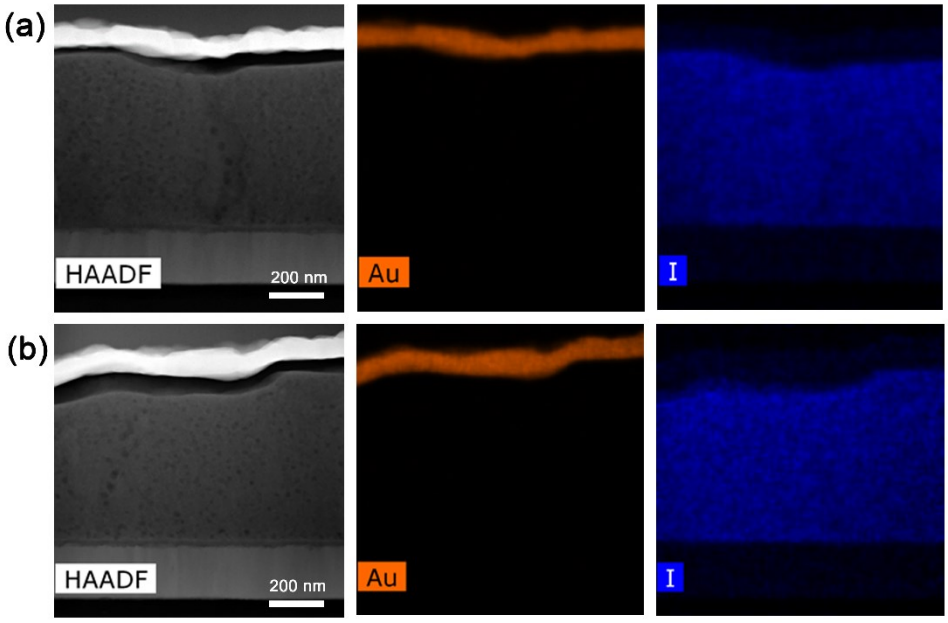

Figure S16. HAADF-STEM images and EDX mapping of Au and iodine of the aged (a) S_1P_0 and (b) S_1P_1 based $Cs_{0.06}FA_{0.58}MA_{0.36}I_{2.88}Br_{0.12}$(Cl) PSCs after 1000 h aging test at 85 °C.

Table S6. Efficient or stable planar structured perovskite solar cells via low temperature preparation process recently published in some journals.

Structure	Journal	Date	Upper charge transport material	PCE	Aging test condition	Normalized PCE	Ref.
Regular (n-i-p)	Nat. Energy	Nov. 2016	spiro-OMeTAD	19.9 %	none	none	3
Regular (n-i-p)	Science	Feb. 2017	spiro-OMeTAD	20.1%	500 h under AM 1.5	90%	4
Inverted (p-i-n)	Nat. Energy	Jun. 2017	C_{60}/BCP	20.59%	35 days, RT in air	100%	5
Regular (n-i-p)	Adv. Mater.	Oct. 2017	spiro-OMeTAD	20.9%	none	none	6
Regular (n-i-p)	Science	Nov. 2017	(Ta-WO_x)/ polymer	21.2%	1000 h under AM 1.5	97%	7
Inverted (p-i-n)	Science	Jun. 2018	PC61BM/C_{60}/BCP	20.90%	500 h at 85 °C	95%	8
Regular (n-i-p)	Nat. Commun.	Aug. 2018	spiro-OMeTAD	21.52%	none	none	9
Inverted (p-i-n)	Nature	Jul. 2019	PCBM/BCP	19.8%	1800h under AM 1.5	95%	10
Regular (n-i-p)	Nat. Photonics	Apr. 2019	spiro-OMeTAD or PTAA	23.32%	500 h 85 °C	80%	11
Regular (n-i-p)	Adv. Mater.	Jul. 2019	spiro-OMeTAD	21.18%	160 h 85 °C	~60%	12
Inverted (p-i-n)	Adv. Mater.	Sep. 2019	C_{60}/BCP	21.6%	MPP 800 h	80%	13
Inverted (p-i-n)	Nat. Energy	Jan. 2020	C_{60}/BCP	22.3%	1000 h at 85 °C	90%	14
Regular (n-i-p)	/	/	SMPHTC	22.7%	1000 h at 85 °C MPP 560 h	90% 92%	**This work**

Reference

1. L. Wang, Y. Huang, A. Waleed, K. Wu, C. Lin, Z. Wang, G. Zheng, Z. Fan, J. Sun and H. Zhou, *ACS Appl. Mater. Interfaces*, 2017, **9**, 25985-25994.
2. L. Wang, H. Zhou, J. Hu, B. Huang, M. Sun, B. Dong, G. Zheng, Y. Huang, Y. Chen and L. Li, *Science*, 2019, **363**, 265-270.
3. Q. Jiang, L. Zhang, H. Wang, X. Yang, J. Meng, H. Liu, Z. Yin, J. Wu, X. Zhang and J. You, *Nat. Energy*, 2016, **2**, 1-7.
4. H. Tan, A. Jain, O. Voznyy, X. Lan, F. P. G. De Arquer, J. Z. Fan, R. Quintero-Bermudez, M. Yuan, B. Zhang and Y. Zhao, *Science*, 2017, **355**, 722-726.
5. X. Zheng, B. Chen, J. Dai, Y. Fang, Y. Bai, Y. Lin, H. Wei, X. C. Zeng and J. Huang, *Nat. Energy*, 2017, **2**, 1-9.
6. Q. Jiang, Z. Chu, P. Wang, X. Yang, H. Liu, Y. Wang, Z. Yin, J. Wu, X. Zhang and J. You, *Adv. Mater.*, 2017, **29**, 1703852.
7. Y. Hou, X. Du, S. Scheiner, D. P. McMeekin, Z. Wang, N. Li, M. S. Killian, H. Chen, M. Richter and I. Levchuk, *Science*, 2017, **358**, 1192-1197.
8. D. Luo, W. Yang, Z. Wang, A. Sadhanala, Q. Hu, R. Su, R. Shivanna, G. F. Trindade, J. F. Watts and Z. Xu, *Science*, 2018, **360**, 1442-1446.
9. D. Yang, R. Yang, K. Wang, C. Wu, X. Zhu, J. Feng, X. Ren, G. Fang, S. Priya and S. F. Liu, *Nat. Commun.*, 2018, **9**, 1-11.
10. S. Bai, P. Da, C. Li, Z. Wang, Z. Yuan, F. Fu, M. Kawecki, X. Liu, N. Sakai and J. T.-W. Wang, *Nature*, 2019, **571**, 245-250.
11. Q. Jiang, Y. Zhao, X. Zhang, X. Yang, Y. Chen, Z. Chu, Q. Ye, X. Li, Z. Yin and J. You, Nat. Photonics, 2019, **13**, 460-466.
12. D. Zheng, R. Peng, G. Wang, J. L. Logsdon, B. Wang, X. Hu, Y. Chen, V. P. Dravid, M. R. Wasielewski and J. Yu, *Adv. Mater.*, 2019, **31**, 1903239.
13. H. Chen, Q. Wei, M. I. Saidaminov, F. Wang, A. Johnston, Y. Hou, Z. Peng, K. Xu, W. Zhou and Z. Liu, *Adv. Mater.*, 2019, **31**, 1903559.
14. X. Zheng, Y. Hou, C. Bao, J. Yin, F. Yuan, Z. Huang, K. Song, J. Liu, J. Troughton and N. Gasparini, *Nat. Energy*, 2020, 1-10.